

Aminocyclopropane Carboxylic Acid Synthase Is a Regulated Step in Ethylene-Dependent Induced Conifer Defense. Full-Length cDNA Cloning of a Multigene Family, Differential Constitutive, and Wound- and Insect-Induced Expression, and Cellular and Subcellular Localization in Spruce and Douglas Fir^{1,2}[W][OA]

Steven G. Ralph³, J.W. Hudgins³, Sharon Jancsik, Vincent R. Franceschi, and Jörg Bohlmann*

Michael Smith Laboratories (S.G.R., J.W.H., S.J., J.B.) and Departments of Botany and Forest Sciences (J.B.), University of British Columbia, Vancouver, British Columbia, Canada V6T 1Z4; and School of Biological Sciences, Washington State University, Pullman, Washington 99164-4236 (J.W.H., V.R.F.)

In conifer stems, formation of chemical defenses against insects or pathogens involves specialized anatomical structures of the phloem and xylem. Oleoresin terpenoids are formed in resin duct epithelial cells and phenolics accumulate in polyphenolic parenchyma cells. Ethylene signaling has been implicated in the induction of these chemical defenses. Recently, we reported the cloning of 1-aminocyclopropane-1-carboxylic acid oxidase (ACO) from spruce (*Picea* spp.) and Douglas fir (*Pseudotsuga menziesii*). ACO protein was constitutively expressed in Douglas fir and only weakly induced upon wounding. We now cloned seven full-length and one near full-length cDNA representing four distinct 1-aminocyclopropane-1-carboxylic acid synthases (ACS; ACS1, ACS2, ACS3, and ACS4) from spruce and Douglas fir. Cloning of ACS has not previously been reported for any gymnosperm. Using gene-specific, quantitative real-time polymerase chain reaction, we measured constitutive expression for the four ACS genes and the single-copy ACO gene in various tissues of Sitka spruce (*Picea sitchensis*) and in white spruce (*Picea glauca*) somatic embryos. ACO and ACS4 were ubiquitously expressed at high levels; ACS1 was predominantly expressed in developing embryos and ACS2 and ACS3 were expressed only at very low levels. Insect attack or mechanical wounding caused strong induction of ACS2 and ACS3 in Sitka spruce bark, a moderate increase in ACO transcripts, but had no effect on ACS1 and ACS4. ACS protein was also strongly induced following mechanical wounding in Douglas fir and was highly abundant in resin duct epithelial cells and polyphenolic parenchyma cells. These results suggest that ACS, but not ACO, is a regulated step in ethylene-induced conifer defense.

Conifers in the pine family (Pinaceae) represent the most economically important forest trees and are

fundamental species to many ecosystems across the northern Hemisphere. Because of their extensive geographic range and often very long life spans of up to several hundred years, conifers are exposed to a wide variety of potential herbivores, such as insects and mammals, as well as to free-living or insect-associated fungal pathogens. In general, conifers demonstrate resistance or tolerance to most herbivores, although some specialized conifer insect pests, such as certain bark beetles and weevils, cause substantial damage and mortality to individual trees and to large conifer forests (Alfaro et al., 2002; Raffa et al., 2005; Seybold et al., 2006).

As a resistance strategy against pathogens and herbivores, conifers have evolved a variety of anatomical and chemical defense systems (Franceschi et al., 2005; Keeling and Bohlmann, 2006). For example, bark tissues in conifer stems can provide a vigorous and effective barrier with chemical defenses (e.g. accumulation of terpenoid oleoresin and phenolics) that are often associated with specialized anatomical or cellular defense structures (e.g. resin ducts, phloem polyphenolic parenchyma [PP] cells, lignified periderm,

¹ This work was supported by the Natural Sciences and Engineering Research Council of Canada, Genome Canada, Genome British Columbia, the province of British Columbia, the Canadian Foundation for Innovation, and the British Columbia Knowledge and Development Funds (grants to J.B.). J.B. is an E.W.R. Steacie Memorial Fellow of the Natural Sciences and Engineering Research Council of Canada.

² This paper is dedicated to the memory of Dr. Vincent R. Franceschi.

³ These authors contributed equally to the paper.

* Corresponding author; e-mail bohlmann@interchange.ubc.ca; fax 604-822-2114.

The author responsible for distribution of materials integral to the findings presented in this article in accordance with the policy described in the Instructions for Authors (www.plantphysiol.org) is: Jörg Bohlmann (bohlmann@interchange.ubc.ca).

[W] The online version of this article contains Web-only data.

[OA] Open Access articles can be viewed online without a subscription.

www.plantphysiol.org/cgi/doi/10.1104/pp.106.089425

scleireids, and calcium oxalate crystals). Following attack by stem-boring insects or fungal pathogens, conifer bark tissues can respond by induced activation or de novo formation of resin duct and PP cells. Induced PP cells appear to mobilize large quantities of vacuolar phenolics and are associated with systemic and acquired resistance (Christiansen et al., 1999; Bonello et al., 2001, 2003; Bonello and Blodgett, 2003; Krokene et al., 2003). To date, only a few studies have reported genes with a potential function in induced PP cell defenses (Nagy et al., 2004; Ralph et al., 2006a, 2006b). In contrast, a considerable amount of information exists on the chemical composition and biochemistry of conifer terpenoids found in constitutive and traumatic resin ducts (TDs; Trapp and Croteau, 2001; Huber et al., 2004; Martin and Bohlmann, 2005; Schmidt et al., 2005; Keeling and Bohlmann, 2006; Phillips et al., 2006), and much is known about the genes and enzymes for these terpenoid defenses (Martin et al., 2004; Ro et al., 2005; Keeling and Bohlmann, 2006). Many conifers accumulate large quantities of diterpene resin acids and monoterpenes in constitutive resin ducts as a preformed defense. Damage from herbivores and pathogens can lead to additional activation of constitutive resin ducts (Ruel et al., 1998) and de novo formation of TDs from the cambial zone (Christiansen et al., 1999; Nagy et al., 2000). The ensuing resin is the result of increased biosynthesis and accumulation in the activated constitutive resin duct and TD systems (Martin et al., 2002; Miller et al., 2005).

Despite the importance of induced terpenoid and phenolic defenses in conifer resistance, relatively little is known about insect- or pathogen-induced signaling events that lead to activation of resin duct and PP cells or their de novo formation. In a series of studies using exogenously applied ethylene (Hudgins and Franceschi, 2004) or methyl jasmonate (MeJA; Franceschi et al., 2002; Martin et al., 2002, 2003; Fäldt et al., 2003; Hudgins et al., 2003, 2004; Huber et al., 2005; Miller et al., 2005), it was demonstrated that both hormones act as elicitors of conifer chemical and cellular defense responses. Recent studies showed that MeJA application can result in increased resistance of Norway spruce (*Picea abies*) against the bark beetle (*Ips typographus*; Erbilgin et al., 2006) and its fungal associate *Ceratocystis polonica* (Zeneli et al., 2006). Miller et al. (2005) and Ralph et al. (2006b) demonstrated that feeding by the white pine weevil induced the accumulation of transcripts of the octadecanoid pathway in Sitka spruce (*Picea sitchensis*). In Douglas fir (*Pseudotsuga menzeisii*) stems, wounding and MeJA application induce ethylene formation, whereas application of the ethylene inhibitor 1-methylcyclopropane reduced MeJA- or wound-induced accumulation of phenolics and TD development (Hudgins and Franceschi, 2004). Together, these studies agree with a model that ethylene acts downstream of octadecanoid signaling in the anatomical and chemical defenses of conifers. Therefore, both octadecanoid and ethylene biosynthesis are relevant

targets for studies on the regulation of induced conifer resistance.

Ethylene is well known for regulating many processes in plant biology, such as cell differentiation, growth, development, reproduction, and response to environmental stress (for review, see Bleecker and Kende, 2000; Klee and Clark, 2004; Nehring and Ecker, 2004; Pech et al., 2004). Ethylene is generated from 1-aminocyclopropane-1-carboxylic acid, which is synthesized by 1-aminocyclopropane-1-carboxylic acid synthase (ACS), and subsequently converted to ethylene by 1-aminocyclopropane-1-carboxylic acid oxidase (ACO). As a first step toward molecular characterization of ethylene formation and regulation in induced conifer defense, we recently cloned ACO full-length (FL)-cDNAs from Douglas fir, white spruce (*Picea glauca*), and Sitka spruce (Hudgins et al., 2006). ACO transcript profiles appear to be dominated by a single gene in these species. ACO protein was constitutively expressed and only weakly induced by wounding in Douglas fir bark and, therefore, is unlikely to be a regulated step in ethylene-dependent induced defense in this system (Hudgins et al., 2006). We therefore decided to further investigate ACS for a possible role in induced conifer defense.

A substantial amount of information exists on ACS in various angiosperm species. However, to our knowledge, cloning and characterization of ACS has not been reported for a gymnosperm. ACS is a cytosolic enzyme that requires pyridoxal phosphate as a cofactor (Bleecker and Kende, 2000). In angiosperms, ACS proteins are encoded by multigene families in all species examined (Liang et al., 1992; Bleecker and Kende, 2000; Pech et al., 2004). For example, sequencing of the Arabidopsis (*Arabidopsis thaliana*) genome revealed an ACS multigene family consisting of 12 members (Arabidopsis Genome Initiative, 2000). Further functional characterization indicates that this gene family represents one pseudogene, eight functional homodimers, one nonfunctional homodimer, and two distant ACS-like genes able to complement *Escherichia coli* aminotransferase mutants, suggesting possible alternative functions for these two genes (Yamagami et al., 2003). It is well established in angiosperms that distinct members of ACS multigene families are differentially regulated by abiotic and biotic stresses (Kende, 1993; Bleecker and Kende, 2000). For example, Tsuchisaka and Theologis (2004) recently demonstrated that in Arabidopsis ACSs are differentially regulated during normal cell development processes and during stresses that included wounding and anaerobic conditions.

Here, we describe the FL-cDNA or near FL-cDNA cloning and sequence characterization of eight ACSs from white spruce, interior spruce (*Picea glauca* × *engelmannii*), and Douglas fir, representing four distinct ACS or ACS-like genes in these conifers. We provide detailed quantitative and gene-specific expression analyses of ACS and ACO transcripts showing differential patterns of spatial and temporal

expression in constitutive as well as wound- and insect-induced Sitka spruce tissues. Using Douglas fir, we demonstrate wound-induced ACS protein expression and show cellular and subcellular localization of ACS in the cytosol of specialized epithelial cells of cortical resin ducts, PP cells, and ray parenchyma cells of wound-induced bark tissue. Our results suggest that ACS is a regulated step in ethylene signaling in induced cellular and chemical defense in conifers.

RESULTS

cDNA Cloning of ACS Genes from Spruce and Douglas Fir

To obtain initial sequence information for ACS genes from conifers, a TBLASTN search of the spruce expressed sequence tag (EST) and FL-cDNA databases of the Treenomix project (Ralph et al., 2006b) was performed using ACS sequences from both tomato (*Lycopersicon esculentum*) and Arabidopsis, which resulted in the identification of nine putative spruce ACS ESTs. A comparison of sequences obtained by complete insert sequencing, combined with 5' RACE to extend truncated cDNAs, indicated that these ESTs represent five unique FL-cDNAs: *PgACS1*, *PgeACS2*, *PgeACS3a*, *PgeACS3b*, and *PgACS4* (Fig. 1; Table I). *PgACS1* was identified as a 1,455-bp transcript from white spruce clone I-1026 and contains 5'- and 3'-untranslated regions (UTRs) of 55 and 40 bp [excluding the poly(A) tail], respectively. Three transcripts were obtained from interior spruce clone Fal-1028: *PgeACS2*, *PgeACS3a*, and *PgeACS3b*. *PgeACS2* consists of a 1,773-bp transcript with 5' and 3' UTRs of 101 and 313 bp, respectively. *PgeACS3a* and *PgeACS3b* are both 1,898 bp in length with 5' and 3' UTRs of 59 and 279 bp, respectively. These transcripts share 99.3% identity at the nucleotide level and 98.5% identity between the translated proteins, suggesting these FL-cDNAs encode allelic variants of the same ACS gene. The final putative spruce ACS gene identified, *PgACS4*, encodes a transcript of 1,730 bp obtained from white spruce clone PG29, with 5' and 3' UTR lengths of 71 and 60 bp, respectively. The translated proteins for all five transcripts are predicted to capture the entire open reading frame (ORF) based on overall similarity to angiosperm ACS proteins and include both a starting Met (all five transcripts) and stop codons upstream within the 5' UTR (all except for *PgACS1*). The predicted ORFs for the five FL-cDNAs range from 447 to 527 amino acids and have predicted pI and molecular mass values ranging from 5.70 to 8.48 and 50.0 to 58.8 kD, respectively (Table I). Pairwise sequence similarities among predicted amino acids of the five putative spruce ACS FL-cDNAs range from 98.5% identity between *PgeACS3a* and *PgeACS3b* to 37.4% identity between *PgACS4* and *PgeACS3a* and *PgeACS3b* (Table II). The remaining five putative spruce ACS ESTs found in the Treenomix database likely represent truncated

forms or splice variants of the five FL-cDNAs described here.

ACS cDNA sequences from Douglas fir were obtained by reverse transcription (RT)-PCR using sets of primers both within the UTRs and at the ORF termini based upon *PgeACS2*, *PgeACS3a*, and *PgACS4* transcripts with two tissue sources as templates; wounded bark (including phloem and cambium) and green shoot tips. These three primer combinations produced distinct PCR products in both tissue sources, which, upon further purification and sequencing of PCR products from the bark RNA template, combined with 5' RACE to extend a truncated *PmACS2* cDNA, provided unique cDNAs of 1,734 (*PmACS2*), 1,907 (*PmACS3*), and 1,687 bp (*PmACS4*; Table I). *PmACS2* possesses 5' and 3' UTRs of 146 and 208 bp, respectively, in length, and when translated encodes a 460-amino acid protein with a predicted pI value of 5.79 and molecular mass of 52.0 kD. *PmACS4* possesses 5' and 3' UTRs of 61 and 36 bp, respectively, in length, and when translated encodes a 530-amino acid protein with a predicted pI value of 7.49 and molecular mass of 58.9 kD. Pairwise sequence alignments of the deduced amino acid sequences indicate that the putative starting Met and stop codon of *PmACS2* overlaps with *PgeACS2*, as does *PmACS4* and *PgACS4*, and stop codons are present upstream within the 5' UTRs of both Douglas fir proteins, suggesting that *PmACS2* and *PmACS4* are FL-cDNAs. The spruce and Douglas fir ACS2 proteins share 84.1% amino acid identity (Table II) and 85.1% nucleotide identity between the overlapping transcript regions. *PgACS4* and *PmACS4* share 85.3% amino acid identity (Table II) and 93.3% nucleotide identity between the overlapping transcript regions. *PmACS3* encodes a predicted protein of 399 amino acids, which, based on pairwise sequence alignment with *PgeACS3a*/*PgeACS3b*, likely represents a truncated ACS protein due to a frameshift. The putative starting Met of *PmACS3* overlaps with that of *PgeACS3a*/*PgeACS3b*; however, the C terminus of *PmACS3* is approximately 130 amino acids shorter than the complete ORF in spruce. Multiple sets of primers were also designed based on the spruce *PgACS1* sequence in an attempt to obtain a related transcript from Douglas fir by RT-PCR, but we were unable to obtain even a partial transcript using bark or green shoot tip tissue as templates. In retrospect, this was likely due to the fact we did not analyze Douglas fir embryonic tissue because *PgACS1* is primarily expressed in spruce embryos (see below).

Sequence Relatedness of Conifer and Angiosperm ACS Proteins

We performed maximum likelihood analysis using 28 ACS protein sequences from spruce, Douglas fir, Arabidopsis, and tomato to analyze the evolutionary relationships between conifer (gymnosperm) and angiosperm ACS genes. Multiple protein sequence alignments were performed using ClustalW and then

manually adjusted to define a conserved sequence of about 430 amino acids. Using the neighbor-joining algorithm, we generated a phylogenetic tree (Fig. 2), which shows that six of the eight conifer ACS proteins form a distinct cluster, suggesting that ACS genes from gymnosperms and angiosperms have diverged significantly over time since separation of these major land plant lineages. Amino acid identity among the five full-length conifer proteins in this group (i.e. excluding PmACS3) ranges from 56.7% to 98.5%, and from 44.7% to 62.7% between these conifer ACS proteins and Arabidopsis ACS proteins (i.e. excluding AtACS10 and AtACS12; Table II). The remaining two conifer ACS proteins, PgACS4 and PmACS4, group more closely with AtACS10 and AtACS12 (Fig. 2), both of which have been demonstrated to complement *E. coli* aminotransferase mutants (Yamagami et al., 2003), suggesting that these Arabidopsis proteins, and possibly PgACS4 and PmACS4 as well, are not true ACS proteins. Amino acid identity between PgACS4/PmACS4, and the two putative Arabidopsis aminotransferases is relatively low (range from 42.8%–46.7%), but still higher than between PgACS4/PmACS4 and true Arabidopsis ACS proteins (range from 31.4%–40.2%) or between PgACS4/PmACS4 and the other five conifer ACS proteins (range from 36.1%–43.2%; Table II). For comparison, amino acid identity among the true Arabidopsis ACS proteins ranges from 46.0% to 91.7% and from 26.0% to 36.4% between the putative aminotransferases and true ACS proteins in Arabidopsis. All spruce ACS isozymes contain the seven conserved boxes (Fig. 1) found in ACSs from other plant species (Yang and Dong, 1993; Yamagami et al., 2003).

Constitutive Transcript Profiles of Spruce ACS and ACO Assessed by Real-Time PCR

The existence of a multigene ACS family in species of spruce and Douglas fir may suggest different roles of individual ACSs in constitutive or induced processes. In an attempt to illustrate possible differences in spatial patterns of RNA expression, the relative constitutive abundance of the four different spruce ACS transcripts (ACS1–ACS4) was quantified using real-time PCR in total RNA isolated from different stem tissues (cortex, phloem, cambium, and xylem), young lateral shoot tips, and root tissues from Sitka spruce. We also measured ACS expression in developing somatic embryos of white spruce. Real-time PCR expression data were normalized to housekeep-

ing gene control levels (i.e. eukaryotic translation initiation factor [TIF]5A). Gene-specific ACS primers were designed based on FL-cDNA sequences for PgACS1, PgeACS2, PgeACS3a/b, and PgACS4.

ACS1 transcript expression was most dominant in developing somatic embryos (Fig. 3A; please note different scale for ACS1 in embryos), with the next most abundant tissue expression in roots at 33.0-fold lower levels than embryos. ACS1 was only marginally detectable in shoots, cortex, phloem, and cambium (about 4 or 5 orders of magnitude lower than TIF5A), with no detectable transcript expression in xylem (Fig. 3A). ACS2 was expressed at moderate to low levels (about 2–4 orders of magnitude lower than TIF5A) in all tissues examined, with highest expression in roots and cortex, and no detectable transcript in xylem. ACS3 showed a pattern of tissue expression similar to that of ACS2, but was present at 5.6- to 30.0-fold lower levels in each tissue (about 4 or 5 orders of magnitude lower than TIF5A), except for developing embryos where ACS2 was only 2.2-fold more abundant (Fig. 3A). ACS3 expression was highest in roots and cortex, with no detectable transcripts in xylem. In contrast to the spatial patterns of transcript abundance for other spruce ACS genes, ACS4 was ubiquitously expressed at high levels (about 1 or 2 orders of magnitude lower than TIF5A) in all tissues, with greatest transcript abundance in the cortex and roots and lowest in developing somatic embryos.

To complement monitoring the spatial distribution of the four spruce ACS transcripts, we also examined transcript levels for ACO, which is the final step in the ethylene biosynthesis pathway and appears to be represented by a single gene in spruce (Hudgins et al., 2006). ACO was ubiquitously expressed at high levels (about 1 or 2 orders of magnitude lower than TIF5A), with the transcript 4.7- to 21.7-fold more abundant in shoots than any other tissues (Fig. 3A).

Induced Transcript Profiles of Spruce ACS and ACO in Response to Mechanical Wounding or Insect Feeding by Weevils Assessed by Real-Time PCR

Having established the spatial patterns of expression for the four ACS and one ACO transcript in spruce, we next examined these genes for a possible role in the wound- and insect-induced defense response of Sitka spruce by assessing their temporal patterns of expression in response to treatment. In brief, 2-year-old Sitka spruce saplings were subjected on their stems to either feeding by adult white pine

Figure 1. Sequence relatedness of conifer and Arabidopsis deduced ACS proteins. Amino acid sequence alignment of predicted ACS proteins from white spruce (PgACS), interior spruce (PgeACS), Douglas fir (PmACS), and Arabidopsis (AtACS) generated using ClustalW (blosum matrix, gap open, and gap extension penalties of 5.0 and 1.0, respectively) and Boxshade. Conserved similarity shading is based on 50% identity (black) and 50% similarity (gray). The seven conserved domains of the ACS proteins are marked as boxes 1 to 7. The 50-amino acid stretch of AtACS2 containing the peptide for antibody generation is indicated by a red dashed line. Nomenclature and GenBank protein accession numbers for all sequences shown in this alignment are provided in Table II.

Table I. Gene name, genotype, protein and transcript features of spruce and Douglas fir ACS genes

n.a., Not applicable.

Clone ID	Gene Name	cDNA Library (1), RACE (2), or cDNA Template Tissue Sources (3)	Species (Genotype)	cDNA Length (bp)	5'-UTR Length (bp)	3'-UTR Length ^a (bp)	ORF Length (Amino Acid)	Protein pI	Protein Molecular Mass (kD)
WS0342_M22	<i>PgACS1</i>	(1) Somatic embryo	<i>P. glauca</i> (<i>Pg</i> ; I-1026)	1,455	55	40	447	5.70	50.0
WS00944_L14	<i>PgeACS2</i>	(1 and 2) MeJA/wounded bark (with phloem and cambium) time course	<i>P. glauca</i> × <i>engelmannii</i> (<i>Pge</i> ; Fal-1028)	1,773	101	313	447	5.93	50.4
WS00956_O07	<i>PgeACS3a</i>	(1) MeJA/wounded bark (with phloem and cambium) time course	<i>P. glauca</i> × <i>engelmannii</i> (Fal-1028)	1,898	59	279	520	6.19	58.1
WS00956_O07	<i>PgeACS3b</i>	(1) MeJA/wounded bark (with phloem and cambium) time course	<i>P. glauca</i> × <i>engelmannii</i> (Fal-1028)	1,898	59	279	520	6.19	58.2
WS00729_O03	<i>PgACS4</i>	(1) Shoots developmental stages (2) Flushing buds	<i>P. glauca</i> (PG29)	1,730	71	60	527	8.48	58.8
DF_WS00944_L14	<i>PmACS2</i>	(2 and 3) Bark tissue (with phloem and cambium) harvested 24 h after wounding	<i>P. menziesii</i> (<i>Pm</i> ; wild)	1,734	146	208	460	5.79	52.0
DF_WS00956_O07	<i>PmACS3^b</i>	(3) Bark tissue (with phloem and cambium) harvested 24 h after wounding	<i>P. menziesii</i> (wild)	1,907	63	n.a.	399	n.a.	n.a.
DF_WS00729_O03	<i>PmACS4</i>	(3) Bark tissue (with phloem and cambium) harvested 24 h after wounding	<i>P. menziesii</i> (wild)	1,687	61	36	530	7.49	58.9

^aExcluding the poly(A) tail. ^bPartial cDNA.

weevils or mechanical wounding using a needle. Transcript profiles were monitored in bark tissues using real-time PCR 2, 6, and 48 h after the onset of treatment and compared to untreated control tissues. Data are presented as transcript abundance normalized to *TIF5A* levels (Fig. 3B) and as fold induction relative to untreated control tissues (Table III). In general, three of the five transcripts examined (i.e. *ACS2*, *ACS3*, and *ACO*) showed statistically significant increases in abundance following mechanical wounding and/or weevil feeding. All three transcript species were rapidly induced and had reached peak levels at 2 h (*ACS2* and *ACS3*) or 6 h (*ACO*), following mechanical wounding. Both *ACS2* and *ACS3* transcripts were expressed at relatively low levels in control bark, with increases of 155.9-fold and 174.2-fold, respectively, 2 h after mechanical wounding (Fig. 3B; Table III). The levels of both transcript species diminished over time, but were still 8.1-fold (*ACS2*) and 3.7-fold (*ACS3*) more abundant than in control tissues 48 h after wounding. In contrast to the temporal pattern of rapid induction following mechanical wounding, induction by weevil feeding was slower and of lower magnitude, with peak induction at 48 h for *ACS2* (48.9-fold) and *ACS3* (27.9-fold; Fig. 3B; Table III). The differing temporal response to insect herbivory and mechanical wounding treatments likely reflects the very slow, but continuous, feeding by stem-boring weevils compared with a single artificial wounding event.

Unlike *ACS2* and *ACS3*, *ACO* transcripts were present at relatively high levels in untreated control bark and showed only a moderate (3.9-fold), although equally rapid, increase in transcript abundance following mechanical wounding that also diminished with time (Fig. 3B; Table III). The response of *ACO* to weevil feeding was less pronounced, with slightly reduced transcript abundance after 2 and 6 h of weevil feeding and only a small increase (2.4-fold) after 48 h.

The two remaining transcript species examined, *ACS1* and *ACS4*, did not follow the above pattern of induction following wounding or insect damage. *ACS1* was expressed at marginally detectable constitutive levels in bark from untreated control trees, with no consistent pattern of altered transcript levels following either treatment (Fig. 3B; Table III). *ACS4* was the most constitutively abundant of the *ACS* and *ACO* transcripts examined in control bark tissue and demonstrated a weak, and not always statistically significant, down-regulation in response to both treatments at all time points (Fig. 3B; Table III).

Wound-Induced Accumulation of ACS Protein and Cellular and Subcellular Localization of ACS in Resin Ducts and PP Cells in Douglas Fir

In previous work (Hudgins and Franceschi, 2004; Hudgins et al., 2006), Douglas fir was established as a system for the study of ethylene signaling in conifer

Table II. Sequence relatedness of plant ACS proteins

Results from pairwise amino acid sequence comparisons using full-length protein sequences are shown as percent identity. ACS nomenclature and GenBank protein accession numbers are as follows: Arabidopsis: AtACS1 (NP_191710), AtACS2 (NP_171655), AtACS4 (NP_179866), AtACS5 (NP_201381), AtACS6 (NP_192867), AtACS7 (NP_194350), AtACS8 (NP_195491), AtACS9 (NP_190539), AtACS10 (NP_564804), AtACS11 (NP_567330), and AtACS12 (NP_199982); white spruce: PgACS1 and PgACS4; interior spruce: PgeACS2, PgeACS3a, and PgeACS3b; Douglas fir: PmACS2 and PmACS4.

Protein Name	a	b	c	d	e	f	g	h	i	j	k	l	m	n	o	p	q	r	
AtACS1	(a)	100																	
AtACS2	(b)	65.2	100																
AtACS6	(c)	59.4	59.0	100															
AtACS4	(d)	47.4	47.2	46.0	100														
AtACS8	(e)	49.9	49.9	48.9	79.3	100													
AtACS5	(f)	47.3	47.5	47.1	73.4	76.6	100												
AtACS9	(g)	47.7	49.5	47.1	74.1	76.9	91.7	100											
AtACS11	(h)	46.3	47.4	48.9	62.0	65.8	64.5	64.5	100										
PgeACS2	(i)	46.5	46.5	46.2	48.0	50.1	47.3	47.7	49.7	100									
PmACS2	(j)	45.4	45.0	44.7	46.7	49.1	45.8	46.0	48.1	84.1	100								
PgeACS3a	(k)	47.5	45.7	47.3	47.9	48.8	46.8	47.6	47.4	68.9	67.0	100							
PgeACS3b	(l)	47.1	46.3	47.3	48.5	49.3	46.8	47.8	47.4	68.9	67.0	98.5	100						
PgACS1	(m)	48.4	48.2	48.3	50.8	54.6	52.2	52.9	53.4	64.3	61.6	56.7	57.1	100					
AtACS7	(n)	47.7	46.1	48.7	51.3	52.7	50.9	51.8	52.5	56.6	54.1	52.5	52.1	62.7	100				
AtACS10	(o)	26.3	26.4	26.0	29.0	29.8	28.9	30.1	27.6	31.0	29.5	28.1	27.8	32.2	30.9	100			
AtACS12	(p)	29.5	30.8	30.1	34.9	35.1	33.9	35.9	34.0	37.4	35.7	34.0	34.2	39.1	36.4	47.7	100		
PgACS4	(q)	33.4	33.6	33.4	36.0	38.6	36.1	35.9	35.8	41.8	40.9	37.4	37.4	43.2	40.2	44.5	46.7	100	
PmACS4	(r)	32.0	32.1	31.4	34.8	37.0	34.9	35.0	34.9	39.9	39.0	36.3	36.1	40.9	39.6	42.8	45.1	85.3	100

defense. ACO protein was shown by western-blot analysis to be constitutively expressed and weakly induced in bark upon wounding and ACO was localized to specialized defense cell types. To complement this previous work on ACO with new work on ACS, we performed western-blot analysis and immunolocalization using polyclonal Arabidopsis anti-ACS antibodies on the same protein samples and tissues previously analyzed for ACO protein. The ACS antibody was raised against an Arabidopsis synthetic peptide matching AtACS2 (Fig. 1), which shares strong sequence homology with conifer ACS1, ACS2, and ACS3 proteins, but has only limited similarity to conifer ACS4 (Santa Cruz Biotechnology).

ACS antibodies showed strong signals with a single band on western blots of protein extracts from wound-induced stem bark, but did not yield protein signals with extracts from nonwounded control tissue (Fig. 4). The molecular mass of the protein detected was approximately 55 kD on SDS-PAGE, consistent with the predicted molecular mass of conifer ACS proteins (Table I). ACS protein was detected at the first time point of the induced samples at 10 h following wounding, and protein levels remained increased relative to controls over the entire time course until 96 h after wounding (Fig. 4). Next, we tested the specific localization of ACS in wound-induced bark tissues. Immunocytochemistry using ACS antibody showed the most extensive presence of ACS in two different cell types associated with terpenoid and phenolic chemical defenses in wounded bark tissues, namely, epithelial cells that line the inner surface of activated cortical resin ducts (Fig. 5A) and active PP cells that are characterized by

their large and densely stained vacuoles (Fig. 5C), respectively. As a negative control, the nonimmune serum did not generate any reproducible labeling of any cell type (Fig. 5B). In wound-induced bark, ACS labeling was also detected in ray parenchyma cells (Fig. 5, C and D). These cells connect the xylem and outer bark via the cambial zone. Labeling was also detected within the cambial zone itself and was found highly abundant in a ray initial captured in mitosis with nearly complete separation of the duplicated set of chromosomes (Fig. 5D). In control sections of noninduced bark tissues, ACS protein was not detected above the background signal in any cell type (data not shown), confirming the results of western-blot analysis.

High-resolution subcellular localization detected ACS protein in the cytoplasm of PP cells (Fig. 5E), but not in the membranes, cell walls, vacuoles, or other organelles. In the lower magnification images shown in Figure 5, C and D, the antibody also appears to label some nuclear regions of ray parenchyma cells; however, this may be a result of vacuole compression of cytoplasm around the nuclear domains.

DISCUSSION

Conifer trees are able to survive hundreds of years and often dominate large ecosystems due to their apparently highly successful defense systems, which protects them against most herbivores and pathogens. Most prominent among the chemical defenses of conifers in the pine family are the constitutive and inducible terpenoid oleoresins (Martin and Bohlmann,

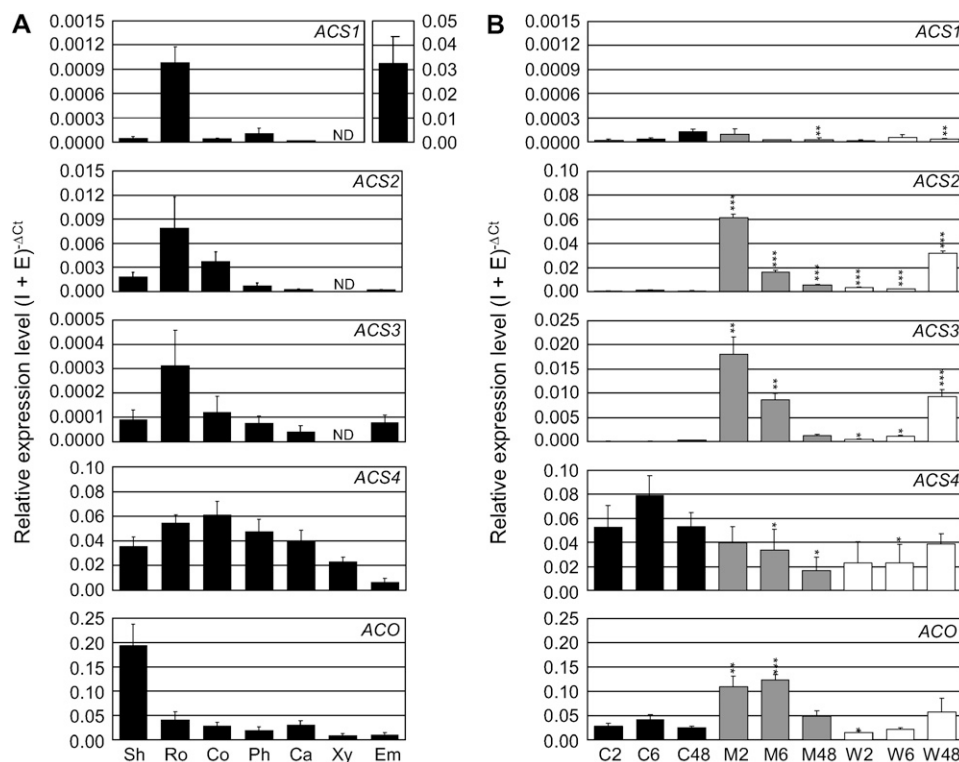


Figure 3. Constitutive and wound- and insect-induced ACS and ACO transcript abundance in spruce tissues. A, Relative abundance of mRNA transcripts of the four distinct spruce ACS genes and the single-copy spruce ACO gene in tissues collected from 2-year-old Sitka spruce trees harvested in May, as well as developing somatic embryos from white spruce. Tissues examined include lateral shoot tips (Sh), roots (Ro), cortex (Co), phloem (Ph), cambium (Ca), xylem (Xy), and embryos (Em). B, Relative abundance of the same four ACS and single ACO transcript species in bark tissues of Sitka spruce trees subjected to mechanical wounding (M), weevil herbivory (W), or left untreated as a control (C), 2, 6, or 48 h after the onset of treatment. A and B, Values obtained by real-time PCR represent mean \pm SE of the mean (SEM; $n =$ three or more independent technical replicates, each consisting of pooled RNA from 10 [A] or five [B] biological replicates) normalized to eukaryotic *TIF5A* (EST IS0013_F24) expression in each tissue by subtracting the Ct value of each transcript, where $\Delta Ct = Ct_{\text{transcript}} - Ct_{\text{TIF5A}}$. Transcript abundance was obtained from the equation $(1 + E)^{-\Delta Ct}$, where E is PCR efficiency, as described by Ramakers et al. (2003). A transcript with relative abundance of 1 is equivalent to the abundance of *TIF5A* in the same tissue. Student's *t* test (two-sample, unpaired, one-sided) was performed to test significance of up- or down-regulation of each transcript between treated and control tissues (*, $P \leq 0.05$; **, $P \leq 0.01$; ***, $P \leq 0.001$). ND, Not detected.

et al., 2006). We therefore extended our previous analysis of ethylene formation in induced conifer defense (Hudgins and Franceschi, 2004; Hudgins et al., 2006) with comprehensive characterization of a multigene ACS family in spruce and Douglas fir. To the best of our knowledge, this study describes the first cDNA cloning, expression analysis, and phylogenetic reconstruction of members of the ACS gene family in any gymnosperm and the first cellular and subcellular protein localization of ACS in plants.

We identified five different ACS cDNA sequences by mining spruce EST and FL-cDNA databases, which, at more than 200,000 sequences, are second only to loblolly pine (*Pinus taeda*) as the largest gymnosperm sequence resource (Ralph et al., 2006b). The five spruce ACS cDNAs represent four clearly distinct ACS genes. These include *PgACS1*, *PgeACS2*, *PgeACS3a*, *PgeACS3b*, and *PgACS4*, with *PgeACS3a* and *PgeACS3b* likely being allelic variants of the same spruce ACS gene (Table I;

Figs. 1 and 2). To extend the previous work on ethylene signaling in Douglas fir (initiated by the late Dr. Vincent Franceschi; Hudgins and Franceschi, 2004; Hudgins et al., 2006), we also cloned three of the corresponding ACSs from this conifer species. Using spruce ACS sequences, we cloned two FL-cDNAs from Douglas fir, *PmACS2*, and *PmACS4*, which are 84% and 85% identical at the amino acid level with spruce ACS2 and ACS4, respectively. A partial cDNA for *PmACS3* was also obtained, which shares high similarity with the spruce ACS3 counterpart. Repeated BLAST searches using the conifer ACS proteins, as well as those from tomato and *Arabidopsis*, against more than 200,000 ESTs and FL-cDNAs from 20 different spruce cDNA libraries representing different tissues, developmental stages, and stress treatments (Ralph et al., 2006b), failed to identify any other ACS-like cDNAs. Considering the depth of this genomic resource, we have likely captured most or all members of the spruce ACS gene family,

Table III. Relative abundance of ACS and ACO transcripts in response to weevil herbivory or mechanical wounding in Sitka spruce bark

Values were determined using real-time PCR and represent fold change relative to untreated control trees (see Fig. 3). Student's *t* test (two-sample, unpaired, one-sided) was performed to test significance (*P*) of up- or down-regulation of each transcript between treated and control tissues. FC, Fold change.

Gene	Mechanical Wounding						Weevil Herbivory					
	2 h		6 h		48 h		2 h		6 h		48 h	
	FC	<i>P</i>	FC	<i>P</i>	FC	<i>P</i>	FC	<i>P</i>	FC	<i>P</i>	FC	<i>P</i>
<i>ACS1</i>	4.3	0.158	0.8	0.367	0.2	0.010	0.7	0.500	1.7	0.308	0.2	0.010
<i>ACS2</i>	155.9	<0.001	12.7	<0.001	8.1	<0.001	7.6	<0.001	1.6	<0.001	48.9	<0.001
<i>ACS3</i>	174.2	0.007	77.1	0.002	3.7	0.088	4.4	0.024	9.7	0.036	27.9	0.001
<i>ACS4</i>	0.8	0.291	0.4	0.044	0.3	0.031	0.4	0.160	0.3	0.017	0.7	0.173
<i>ACO</i>	3.9	0.007	3.0	<0.001	2.0	0.055	0.5	0.042	0.5	0.061	2.4	0.138

with the possible exception of ACS genes that may be expressed at very low levels or exhibit highly selective tissue- or cell-specific expression and therefore might not be captured in the spruce EST collection.

Phylogenetic comparison of the spruce and Douglas fir ACS protein sequences with angiosperm ACS proteins demonstrates that conifers ACS1, ACS2, and ACS3 are relatively closely related to the majority of previously known and functionally characterized angiosperm ACSs (Fig. 2). Within this larger group of gymnosperm and angiosperm proteins, the conifer (gymnosperm) ACS forms a distinct cluster. This topology of the ACS tree suggests that angiosperm and gymnosperm ACSs share a common ancestor and multiple ACS forms evolved by gene duplication and sequence divergence in both lineages after the separation of angiosperms and gymnosperms. Like Arabidopsis, both spruce and Douglas fir also have more distantly related ACS-like proteins (i.e. PgACS4 and PmACS4). The Arabidopsis AtACS10 and AtACS12 proteins have been tentatively classified as aminotransferases (Yamagami et al., 2003) and it is possible that the conifer ACS4 proteins may have similar functions.

Unlike the apparently single-copy conifer ACO gene (Hudgins et al., 2006), multiple ACS genes in spruce and Douglas fir provide possible points of differential regulation of induced ethylene formation, which was previously shown to be involved in induced conifer defense (Hudgins and Franceschi, 2004), or they may have tissue-specific roles. Constitutive expression of the four ACS genes and the single ACO gene reveals a combinatorial pattern of spatial coexpression among the various gene family members. Three ACS transcripts, ACS1, ACS2, and ACS3, were present at low to very low levels in most noninduced tissues examined, with the highest expression in roots and no detectable transcripts in xylem (Fig. 3A). An exception to this pattern of apparently low constitutive expression of these ACS genes was the relatively high abundance of ACS1 transcripts in developing white spruce somatic embryos. In contrast to ACS1, ACS2, and ACS3, the ACS4 gene, which has highest sequence similarity to putative Arabidopsis aminotransferases, was ubiqui-

tously expressed at moderate to high levels in all noninduced Sitka spruce tissues. Similarly, ACO was also highly expressed in all tissues, with the highest expression in young shoot tips. These findings clearly show unique as well as partly overlapping patterns of expression among ACS gene family members and ACO in different conifer tissues. Low expression levels of ACS1, ACS2, and ACS3 make these possible rate-limiting steps in constitutive processes of normal growth and development regulated by ethylene in concert with other phytohormones.

To test whether all four conifer ACS genes are associated with induced defense, we examined transcript abundance in response to both mechanical wounding and weevil feeding over a time course of 2 to 48 h in Sitka spruce bark tissues (Fig. 3B). ACS1 was expressed at very low levels in control bark tissue, with only minor fluctuations in abundance following mechanical wounding or insect feeding. A similar pattern was seen with ACS4, which was abundantly expressed in both treated and control bark. In contrast, ACS2 and ACS3 were rapidly (2 h) and strongly (>150-fold) induced following mechanical wounding, with a similar, although slower, response to weevil feeding.

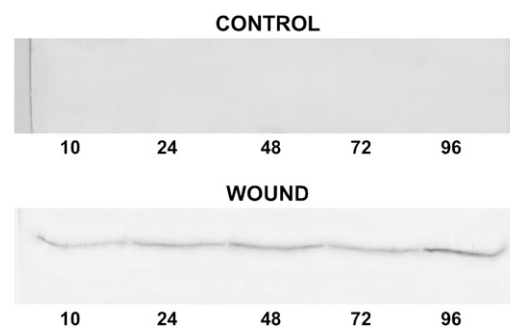


Figure 4. Wound-induced ACS accumulation in protein extracts of Douglas fir bark. ACS western-blot analysis of total protein extracts of control and wound-induced bark at 10, 24, 48, 72, and 96 h posttreatment. A total of 15 μ g protein was loaded per lane, separated by SDS-PAGE, blotted onto a nitrocellulose membrane, and probed with Arabidopsis anti-ACS antibody. Independent repetitions of western-blot analysis showed the same protein profiles.

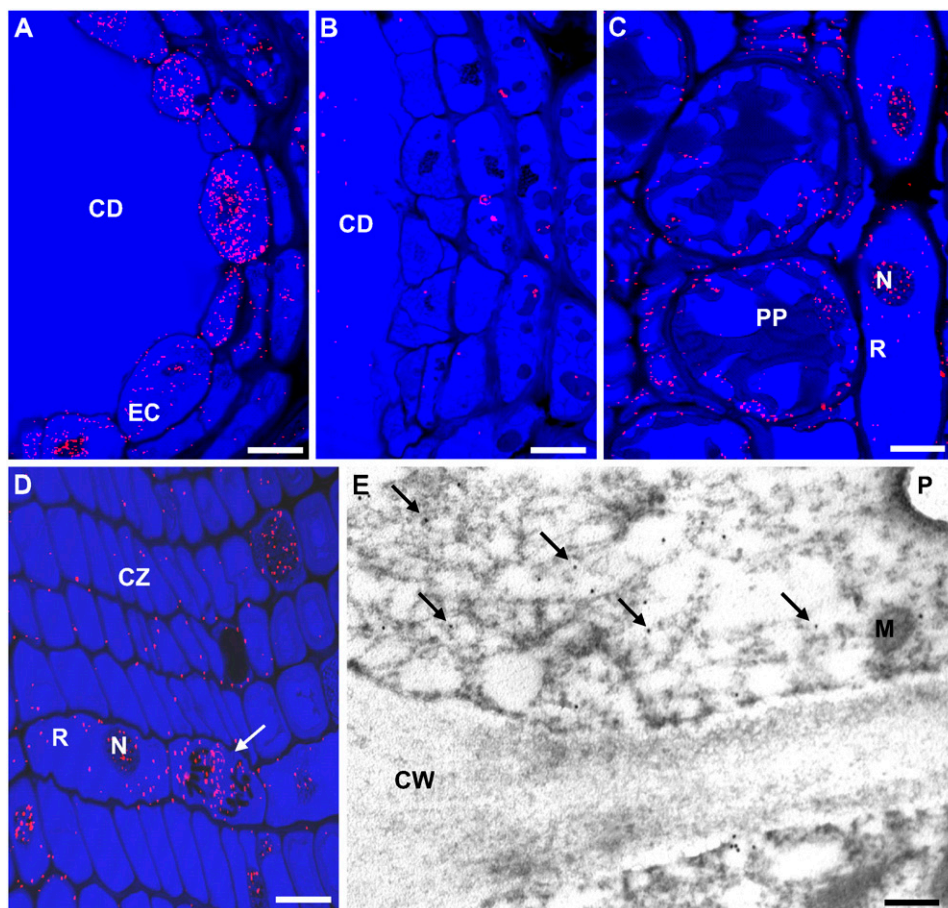


Figure 5. Localization of ACS protein in resin duct epithelial cells, PP cells, and ray parenchyma in wound-induced Douglas fir bark. A to D, ACS immunocytochemical localization in wound-induced bark by confocal microscopy 24 h after wounding. Reflected/transmitted images are of silver-enhanced gold labeling (pink particles). CD, Lumen of cortical resin duct lined by epithelial cells; CW, cell wall; EC, resin duct epithelial cell; M, mitochondria; P, plastid; R, ray parenchyma cell; N, nucleus; CZ, cambial zone. ACS labeling is abundant in resin duct epithelial cells (A), PP cells (C), and ray parenchyma cells (C and D) in the phloem and cambial zone. Note abundance of ACS labels in ray parenchyma initially undergoing mitosis (indicated by white arrow). Bar = 40 μM (A–D). B, Section of resin duct with epithelial cells treated with nonimmune serum. E, Subcellular localization of ACS by transmission electron microscopy. Cross section of wounded tissue showing ACS label occurs within cytoplasmic regions of a PP cell. Bar = 0.75 μM . Examples of labeling are indicated by black arrows.

Interestingly, both of these transcripts were present at low levels in untreated control bark, as well as all other tissues examined for constitutive expression, suggesting that *ACS2* and *ACS3* genes likely function in the regulation of induced ethylene signaling in conifer defense (Hudgins and Franceschi, 2004), whereas such a role seems less obvious for *ACS1* or *ACS4*. In contrast to the *ACO* gene, which is present with relatively high constitutive transcript levels in noninduced bark, the two *ACS* genes, *ACS2* and *ACS3*, with their very low constitutive transcript levels in noninduced bark, could also function as rate-limiting steps in ethylene formation in conifer bark defense.

Western-blot analysis confirmed strong induction of ACS at the protein level in Douglas fir bark following wounding (Fig. 4), consistent with *ACS* transcript accumulation in Sitka spruce and also with previous findings of wound-induced ethylene evolution in this

system (Hudgins and Franceschi, 2004). Unlike *ACO* protein, which was previously shown to be detectable in noninduced bark tissue and only weakly induced (Hudgins et al., 2006), ACS protein was undetectable in untreated control tissue and strongly induced in wounded bark (Fig. 4) using the exact same Douglas fir protein extracts and the exact same immunoblotting procedures as previously applied for *ACO* detection. Data obtained for *ACS* and *ACO* transcripts from induced Sitka spruce bark and protein data obtained for ACS (this study) and *ACO* (Hudgins et al., 2006) in Douglas fir support a model according to which ACS is more likely rate-limiting and more tightly regulated than *ACO* in induced defense. A role of induced ACS protein in the chemical and cellular defense of conifers, in particular, the induced terpenoid resin defense associated with resin duct activation and induced phenolic defense associated with PP cell activation, is

further supported by highly cell-specific localization of ACS to resin duct epithelial cells and PP cells in wound-induced Douglas fir bark (Fig. 5). Induced ACS protein colocalizes with ACO (Hudgins and Franceschi, 2004; Hudgins et al., 2006) to the same defense-related specialized cell types.

In conclusion, rapid accumulation of transcripts and proteins for enzymes involved in ethylene biosynthesis following wounding or insect feeding in conifer bark tissues supports the importance of this phytohormone in signaling inducible defense responses in conifer bark. The previously demonstrated high constitutive expression of ACO protein in conifer bark and its weak inducibility following wounding (Hudgins and Franceschi, 2004; Hudgins et al. 2006), combined with similar observations for ACO transcripts in this study, suggests that ACO is not likely a rate-limiting step in inducible ethylene production in conifer bark tissues. In contrast, we established here that (1) three different spruce ACS transcripts are present at low constitutive levels in conifer bark; (2) ACS protein was not detectable in constitutive conifer bark; (3) two spruce ACS transcripts as well as the Douglas fir ACS protein are strongly inducible by insect feeding and/or mechanical wounding. Together, these results suggest that ACS is a regulated step in wound-induced ethylene synthesis in conifer bark.

MATERIALS AND METHODS

Plant and Insect Materials and Treatments

Three-year-old Douglas fir (*Pseudotsuga menziesii*) saplings were from a commercial nursery (Lawyer Nursery). Growth conditions and details of treatment and tissue harvest of Douglas fir for ACS protein expression and immunolocalization were exactly as previously described (Hudgins et al., 2006). To obtain ACS cDNA clones from Douglas fir, we used two tissue sources: (1) bark tissue (including phloem and cambium) of 2-year-old saplings grown outside at the University of British Columbia (UBC) South Campus farm harvested in June, 2002, 24 h after wound treatment (bark was cut horizontally at 5-mm intervals on opposite sides along the entire length of the stem); and (2) green shoot tips harvested in July, 2002 from lateral branches of a 20-year-old tree grown outside at the UBC South Campus farm. To obtain ACS cDNA clones from species of spruce, we utilized four tissue sources: (1) bark tissue (including phloem and cambium) of 2-year-old interior spruce (*Picea glauca* × *engelmannii*) trees (clone Fal-1028) grown in the UBC greenhouse and harvested in May, 2002, 32 d after wound treatment as described above, and treatment with 0.01% (v/v) MeJA in a 0.1% Tween20 solution applied by spraying along the stem; (2) outer xylem tissue of 2-year-old interior spruce trees grown in the UBC greenhouse and harvested in May, 2002, 48 h after wounding and MeJA treatment (as above); (3) flushing buds from 25-year-old white spruce (*Picea glauca*) trees (clone PG29) grown outside at the Kalamalka Research Station in Vernon, British Columbia, Canada and harvested in May, 2001; and (4) outer xylem harvested in July, 2001 from the same 25-year-old trees. All tissues were flash frozen in liquid nitrogen and stored at -80°C .

To monitor spruce ACS transcript expression in response to wounding or insect attack, Sitka spruce (*Picea sitchensis*) trees (clone FB3-425; derived from somatic embryogenesis [CellFor]) were grown outside at the UBC greenhouse as described by Ralph et al. (2006a) to a height of 60 to 70 cm. Adult white pine weevils (*Pissodes strobi*) were generously provided by Dr. Rene I. Alfaro (Pacific Forestry Centre, Canadian Forest Service). Weevils were reared from larvae in infested Sitka spruce shoots collected at natural infestation sites in British Columbia in 2002 and maintained on Sitka spruce shoots. Two weeks prior to experiments in May, 2003, 2-year-old trees were moved inside the UBC greenhouse and maintained as described by Ralph et al. (2006a). For

mechanical wounding, the bark of five trees per time point was pierced, using an 18-gauge hypodermic needle, at 5-mm intervals on opposite sides along the entire length of the stem. For insect treatment, weevils were kept without food on moist filter paper for 48 h prior to placing them on trees. Insects were caged under mesh bags on the upper two-thirds of the stem (10 weevils on each of five individual trees per time point). For the untreated control, an additional five trees per time point were covered with mesh bags, but otherwise left untreated. Trees were kept in separate treatment groups in a well-ventilated greenhouse. Five trees each for control, wounding, and insect treatments were harvested 2, 6, and 48 h after initiation of treatment. To harvest bark tissue, the upper two-thirds of the tree (excluding the green shoot tip) was cut longitudinally with a razor blade and the outer tissue was peeled off the woody inner stem tissues. For tissue profiling of constitutive ACS expression, cortex, phloem, cambium, and developing xylem were rapidly separated under a dissecting microscope (15 min/tree), along with young lateral shoots and roots, from 10 3-year-old Sitka spruce saplings in May, 2004 and pooled by tissue. White spruce (clone I-1026) somatic embryos for profiling of constitutive ACS expression were generously provided by Dr. David Ellis (CellFor) and grown from callus tissue on medium supplemented with abscisic acid and indole-3-butyric acid for 6 weeks using standard procedures prior to harvest. All tissues used for real-time PCR analysis were flash frozen in liquid nitrogen and stored at -80°C prior to total RNA isolation.

RNA Isolation and cDNA Synthesis

Total RNA was isolated from all tissues, except for somatic embryos, according to the protocol of Kolosova et al. (2004). Total RNA from somatic embryos was isolated using the RNAqueous Midi kit (Ambion) according to the manufacturer's instructions. Total RNA was quantified and quality checked by spectrophotometer and agarose gel. RNA was also evaluated for integrity and the presence of contaminants using RT with SuperScript II reverse transcriptase (Invitrogen) with an oligo (dT)₁₈ primer and αP^{32} dGTP incorporation. After removal of unincorporated nucleotides using gel filtration columns (Microspin S-300 HR columns; Amersham-Pharmacia Biotech), the resulting cDNA smear was resolved using a vertical 1% agarose alkaline gel and visualized using a Storm 860 phosphor imager (Amersham-Pharmacia Biotech).

Isolation of Spruce and Douglas Fir ACS Full-Length cDNA Clones

A TBLASTN search of the Treenomix spruce ESTs and the FL-cDNA database (Ralph et al., 2006b), containing 147,146 ESTs derived from 3'-end sequencing, was performed using ACS sequences from tomato (*Lycopersicon esculentum*) and Arabidopsis (*Arabidopsis thaliana*) to identify nine putative spruce ACS ESTs. CAP3 sequence assembly software (Huang and Madan, 1999) was used to group ESTs into five unique singletons and contigs (40 bp overlap, 95% identity). ACS clones in the pBluescript II SK (+) vector were identified in our cDNA library glycerol stocks, insert sized using PCR with $-21\text{M}13$ forward and M13 reverse primers, and cDNA inserts were sequenced from both ends using the same primers (see Supplemental Table S1 for all primer sequences used in this study). In this manner, the complete FL-cDNA sequence for white spruce (*PgACS1*) was obtained, and partial cDNA sequences were determined for four spruce ACSs. To obtain full-length clones for interior spruce (*PgeACS2*) and *PgACS4*, the FirstChoice RNA ligase-mediated (RLM)-RACE system (Ambion) was used to generate 5'-RACE PCR templates from wounded and MeJA-treated interior spruce bark and xylem tissues, as well as white spruce flushing buds and xylem tissues, according to the manufacturer's instructions. PCR reactions were performed using 1 μL of RACE template, 200 μM each dNTP, 4 mM Tris-HCl (pH 9.0), 20 mM KoAC, 0.6 mM MgSO_4 , 1.25 units of SuperTaq Plus polymerase (Ambion), and 0.4 μM each of the outer RACE forward primer and a gene-specific outer reverse primer in a final volume of 50 μL . The following standard thermal profile was used for all RACE PCRs: 94°C for 3 min; 35 cycles of 94°C for 30 s; 60°C or 52°C for 30 s; and 68°C for 60 s; then 68°C for 7 min. A second nested RACE-PCR was then performed using the same conditions as above, except with 1 μL of the first-round RACE-PCR product as template and the inner RACE forward primer and a gene-specific inner reverse primer. Gene-specific RACE primers used for *PgeACS2* and *PgACS4* were WS00944_L14_RACE_OUTER and WS00944_L14_RACE_INNER and WS00729_O03_RACE_OUTER and WS00729_O03_RACE_INNER, respectively (Supplemental Table S1). PCR

products were cloned into pCR2.1-TOPO vector (Invitrogen) and transformed into *Escherichia coli* electroMAX DH10B cells (Invitrogen). Single colonies were isolated, plasmid DNA sequenced using -21M13 forward and M13 reverse primers, and the resulting sequences organized into contigs to obtain the full-length *PgeACS2* and *PgACS4* sequences. Complete insert sequencing of clone WS00956_O07 identified a potential FL-cDNA with a stop codon that disrupted the most likely ORF. Using this sequence information, WS00956_O07_F1 and WS00956_O07_R1 primers were designed (Supplemental Table S1) and a PCR reaction was performed using 0.1 ng of plasmid from the amplified cDNA library IS-B-A-4 (Ralph et al., 2006b) as template, 200 μM each dNTP, 10 mM Tris-HCl (pH 9.0), 50 mM KoAC, 1.5 mM MgSO_4 , 1 unit of SuperTaq Plus polymerase (Ambion), and 0.5 μM of each primer in a final volume of 20 μL . The thermal profile used for PCR was 95°C for 2 min; 35 cycles of 95°C for 15 s; 60°C or 52°C for 30 s; and 68°C for 2 min; then 68°C for 10 min. The resulting PCR products were cloned and sequenced as described above to yield two highly similar FL-cDNAs, *PgeACS3a* and *PgeACS3b*.

To clone ACS cDNAs from Douglas fir, 15 μg total RNA from wounded bark and green shoot tips were treated with DNaseI (Invitrogen) according to the manufacturer's instructions, followed by RT using SuperScript II reverse transcriptase (Invitrogen) with an oligo(dT)₁₈ primer according to the manufacturer's instructions. Efficiency of cDNA synthesis was assessed by gel electrophoresis. For PCR, primers were designed within the UTR and at the ORF termini based upon *PgeACS2* (DF_WS00944_L14_F1 and DF_WS00944_L14_R2; DF_WS00944_L14_INT1 and DF_WS00944_L14_R1), *PgeACS3a* (WS00956_O07_F1 and WS00956_O07_R1), and *PgACS4* (DF_WS00729_O03_F1 and DF_WS00729_O03_R1; DF_WS00729_O03_F2 and DF_WS00729_O03_R2; Supplemental Table S1). PCR reactions were performed using 100 ng of cDNA template, 200 μM each dNTP, 10 mM Tris-HCl (pH 9.0), 50 mM KoAC, 1.5 mM MgSO_4 , 1 unit of SuperTaq Plus polymerase (Ambion), and 0.5 μM of each primer in a final volume of 20 μL . The following standard thermal profile was used for all PCRs: 95°C for 2 min; 35 cycles of 95°C for 15 s; 60°C or 52°C for 30 s; and 68°C for 2 min; then 68°C for 10 min. PCR products were cloned into pCR2.1-TOPO vector (Invitrogen) and transformed into *E. coli* electroMAX DH10B cells (Invitrogen). Single colonies were isolated, plasmid DNA sequenced using -21M13 forward and M13 reverse primers, and additional primers designed to internal sequences (WS00956_O07_R3, DF_WS00729_O03_INT1, and DF_WS00729_O03_INT2) to yield the FL-cDNA Douglas fir *PmACS4* and partial cDNAs *PmACS2* and *PmACS3*. To obtain a FL-cDNA clone for *PmACS2*, the FirstChoice RLM-RACE system (Ambion) was used to generate a 5'-RACE PCR template from wounded bark as described above. Gene-specific primers for *PmACS2* were DF_WS00944_L14_RACE_OUTER and DF_WS00944_L14_RACE_INNER (Supplemental Table S1). PCR products were cloned into pCR2.1-TOPO vector (Invitrogen) and transformed into *E. coli* electroMAX DH10B cells (Invitrogen). Single colonies were isolated and plasmid DNA sequenced using -21M13 forward and M13 reverse primers to yield the FL-cDNA *PmACS2*.

Sequence and Phylogenetic Analysis

Predictions for pI and molecular mass were made using the entire ORF and the pI/Mw tool at ExPasy (www.expasy.org/tools/pi_tool.html). Amino acid multiple sequence alignments were made with ClustalW (www.ebi.ac.uk/clustalw) and Boxshade (bioweb.pasteur.fr/seqanal/interfaces/boxshade.html) and manually adjusted to define a conserved ACS sequence of approximately 430 amino acids prior to maximum likelihood analysis using Phylml, version 2.4.1 (Guindon and Gascuel, 2003) with the JTT (Jones et al., 1992) amino acid substitution matrix. The proportion of invariant sites as well as the α -shape parameter were estimated by Phylml. Trees were generated using BIONJ (Gascuel, 1997), a modified neighbor-joining algorithm. SEQBOOT of the Phylip, version 3.62 package (Felsenstein, 1993; distributed by the author, Department of Genetics, University of Washington, Seattle; evolution.genetics.washington.edu/phyml.html) was used to generate 100 bootstrap replicates, which were then analyzed using Phylml and the previously estimated parameters. CONSENSE, also from Phylip, was used to create a consensus tree. Treeview (Page, 1996) was used to visualize all trees. Bootstrap values above 50% were added to the maximum likelihood tree generated from the original dataset.

Real-Time PCR Gene Expression and Data Analysis

For constitutive tissue expression profiling, 9 μg of total RNA from each tissue was treated with DnaseI (Invitrogen), divided into three aliquots of 3 μg

each, and independent cDNA synthesis reactions were performed using SuperScript II reverse transcriptase (Invitrogen) with an oligo(dT)₁₈ primer according to the manufacturer's instructions. For analysis of induced tissues, 3 μg of total RNA were pooled from each of five trees for each treatment and time point, treated with DNaseI, divided into three aliquots of 5 μg , and converted to cDNA in three independent reactions. Efficiency of each cDNA synthesis was assessed individually by gel electrophoresis. Gene-specific PCR primers were designed (Supplemental Table S1) using a stringent set of criteria, including predicted melting temperature of $64^\circ\text{C} \pm 2^\circ\text{C}$, primer lengths of 20 to 24 nucleotides, guanine-cytosine content of 40% to 60%, and PCR amplicon lengths of 110 to 280 bp. Primer specificity (single product of expected length) was confirmed by analysis on 2% agarose gel, by melting curve analysis, and for at least one PCR reaction per gene, by sequence verification of PCR amplicons. Primers for spruce eukaryotic *TIF5A* (GenBank accession no. DR448953; EST IS0013_F24) served as a quantification control. PCR was performed in optical 96-well plates with a DNA Engine Opticon2 continuous fluorescence detector (MJ Research) using SYBR Green to monitor double-strand DNA synthesis. Reactions contained 7.5 μL DyNamo HS SYBR Green quantitative PCR kit master mix (Finnzymes), 10 ng cDNA, and 0.3 μM of each primer in a final volume of 15 μL . Reactions with the cDNA template replaced by nuclease-free water or 10 ng of non-reverse-transcribed RNA were run with each primer pair as a control. The following standard thermal profile was used for all PCRs: 95°C for 15 min; 40 cycles of 95°C for 15 s; 60°C for 30 s; and 72°C for 30 s; then 72°C for 10 min. The fluorescence signal was captured at the end of each cycle and melting curve analysis was performed from 65°C to 95°C with data capture every 0.2°C during a 1-s hold. Data were analyzed using Opticon Monitor analysis software, version 2.02 (MJ Research). Quantification of each transcript in each cDNA source consisted of at least three independent (different 96-well plates) technical replicates. To generate a baseline-subtracted plot of the logarithmic increase in fluorescence signal (ΔRn) versus the cycle number, baseline data were collected between cycles 3 and 10. All amplification plots were analyzed with an Rn threshold of 0.003 to obtain threshold cycle (Ct) values. Transcript abundance was normalized to *TIF5A* by subtracting the Ct value of *TIF5A* from the Ct value of each transcript, where $\Delta\text{Ct} = \text{Ct}_{\text{transcript}} - \text{Ct}_{\text{TIF5A}}$. Average \pm SEM Ct values for *TIF5A* in the wound- and weevil-induced tissues and the constitutive tissues were 17.69 ± 0.20 and 17.66 ± 0.21 , respectively. Transcript abundance in control and treated samples was obtained from the equation $(1 + E)^{-\Delta\text{Ct}}$, where E is PCR efficiency, as described by Ramakers et al. (2003), which is derived from the log slope of the fluorescence versus cycle number in the exponential phase of each amplification plot and the equation $(1 + E) = 10^{\text{slope}}$. PCR efficiency for all primer pairs ranged from 90.5% to 95.0%. A transcript with a relative abundance of 1 is equivalent to the abundance of *TIF5A* in the same tissue.

Western-Immunoblot Analysis and Immunocytochemistry

Procedures for protein extractions from the 3-year-old Douglas fir saplings, western-blot analysis, microscopy, and immunocytochemistry were exactly as described in Hudgins et al. (2006). A 1:500 dilution of an affinity-purified polyclonal anti-Arabidopsis ACS (aA-20), raised in goat against a 20-amino acid peptide mapping between amino acid positions 100 and 150 of AtACS2; Santa Cruz Biotechnology) was used for immunoblot analysis. Amino acid sequence analysis indicated that the ACS peptide used for antibody generation shares significant homology with PgACS1 (60% identity, 75% similarity; ACS1 was not identified in Douglas fir), PmACS2 (35% identity, 55% similarity), and PmACS3 (40% identity, 55% similarity), but not PmACS4 (25% identity, 35% similarity). For immunocytochemistry, primary antibody incubation was with the same anti-ACS polyclonal antibody diluted 1:75.

Sequence data from this article can be found in the GenBank/EMBL data libraries under accession numbers EF179148 (*PgACS1*), EF179149 (*PgeACS2*), EF179150 (*PgeACS3a*), EF179151 (*PgeACS3b*), EF179152 (*PgACS4*), EF179153 (*PmACS2*), EF179154 (*PmACS3*), and EF179155 (*PmACS4*).

Supplemental Data

The following materials are available in the online version of this article.

Supplemental Table S1. Primer sequences used for cDNA cloning and real-time PCR.

ACKNOWLEDGMENTS

We thank Dr. Barry Jaquish, Dr. John King, and Dr. Alvin Yanchuk from the British Columbia Ministry of Forests for access to white spruce and Sitka spruce trees, and Dr. David Ellis, CellFor Inc., for interior spruce seedlings and spruce somatic embryos; Dr. Rene I. Alfaro from the Canadian Forest Service for access to white pine weevils; Dr. Kim Rensing for technical assistance with spruce tissue sectioning, Mr. Ian Cullis for somatic embryo propagation, and Mr. David Kaplan for greenhouse support. Confocal and TEM microscopy was performed in the WSU Electron Microscopy Center.

Received September 3, 2006; accepted November 17, 2006; published November 22, 2006.

LITERATURE CITED

- Alfaro RI, Borden JH, King JN, Tomlin ES, McIntosh RL, Bohlmann J (2002) Mechanisms of resistance in conifers against shoot infesting insects. In MR Wagner, KM Clancy, F Lieutier, TD Paine, eds, *Mechanisms and Deployment of Resistance in Trees to Insects*. Kluwer Academic Press, Dordrecht, The Netherlands, pp 101–126
- Arabidopsis Genome Initiative (2000) Analysis of the genome sequence of the flowering plant *Arabidopsis thaliana*. *Nature* **408**: 796–815
- Bleeker AB, Kende H (2000) Ethylene: a gaseous signal molecule in plants. *Annu Rev Cell Dev Biol* **16**: 1–18
- Bonello P, Blodgett JT (2003) *Pinus nigra-Sphaeropsis sapinea* as a model pathosystem to investigate local and systemic effects of fungal infection of pines. *Physiol Mol Plant Pathol* **63**: 249–261
- Bonello P, Gordon TR, Storer AJ (2001) Systemic induced resistance in Monterey pine. *For Pathol* **31**: 99–106
- Bonello P, Storer AJ, Gordon TR, Wood DL, Heller W (2003) Systemic effects of *Heterobasidion annosum* on ferulic acid glucoside and lignin of presymptomatic ponderosa pine phloem, and potential effects on bark-beetle-associated fungi. *J Chem Ecol* **29**: 1167–1182
- Christiansen E, Franceschi VR, Nagy NE, Krokling T, Berryman AA, Krokene P, Solheim H (1999) Traumatic resin duct formation in Norway spruce after wounding or infection with a bark beetle-associated blue-stain fungus *Ceratocystis polonica*. In F Lieutier, WJ Mattson, MR Wagner, eds, *Physiology and Genetics of Tree-Phytophage Interactions*. Les Colloques de l'INRA, INRA Editions, Versailles, France, pp 77–89
- Erbilgin N, Krokene P, Christiansen E, Zeneli G, Gershenson J (2006) Exogenous application of methyl jasmonate elicits defenses in Norway spruce (*Picea abies*) and reduces host colonization by the bark beetle *Ips typographus*. *Oecologia* **148**: 426–436
- Fäldt J, Martin D, Miller B, Rawat S, Bohlmann J (2003) Traumatic resin defense in Norway spruce (*Picea abies*): methyl jasmonate-induced terpene synthase gene expression, and cDNA cloning and functional characterization of (+)-3-carene synthase. *Plant Mol Biol* **51**: 119–133
- Franceschi VR, Krokling T, Christiansen E (2002) Application of methyl jasmonate on *Picea abies* (Pinaceae) stems induces defense-related responses in phloem and xylem. *Am J Bot* **89**: 578–586
- Franceschi VR, Krokene P, Christiansen E, Krokling T (2005) Tansley review: anatomical and chemical defenses of conifer bark against bark beetles and other pests. *New Phytol* **167**: 353–376
- Gascuel O (1997) BIONJ: an improved version of the NJ algorithm based on a simple model of sequence data. *Mol Biol Evol* **14**: 685–695
- Guindon S, Gascuel O (2003) A simple, fast, and accurate algorithm to estimate large phylogenies by maximum likelihood. *Syst Biol* **52**: 696–704
- Huang X, Madan A (1999) CAP3: a DNA sequence assembly program. *Genome Res* **9**: 868–877
- Huber DPW, Philippe RN, Madilao L, Sturrock RN, Bohlmann J (2005) Changes in anatomy and terpene chemistry in roots of Douglas-fir seedlings following treatment with methyl jasmonate. *Tree Physiol* **25**: 1075–1083
- Huber DPW, Ralph S, Bohlmann J (2004) Genomic hardwiring and phenotypic plasticity of terpenoid-based defenses in conifers. *J Chem Ecol* **30**: 2399–2418
- Hudgins JW, Christiansen E, Franceschi VR (2003) Methyl jasmonate induces changes mimicking anatomical defenses in diverse members of the Pinaceae. *Tree Physiol* **23**: 361–371
- Hudgins JW, Christiansen E, Franceschi VR (2004) Induction of anatomically based defense responses in stems of diverse conifers by methyl jasmonate: a phylogenetic perspective. *Tree Physiol* **24**: 251–264
- Hudgins JW, Franceschi VR (2004) Methyl jasmonate-induced ethylene production is responsible for conifer phloem defense responses and reprogramming of stem cambial zone for traumatic resin duct formation. *Plant Physiol* **135**: 2134–2149
- Hudgins JW, Ralph SG, Franceschi VR, Bohlmann J (2006) Ethylene in induced conifer defense: cDNA cloning, protein expression, and cellular and subcellular localization of 1-aminocyclopropane-1-carboxylate oxidase in resin duct and phenolic parenchyma cells. *Planta* **224**: 865–877
- Jones DT, Taylor WR, Thornton JM (1992) The rapid generation of mutation data matrices from protein sequences. *Comput Appl Biosci* **8**: 275–282
- Keeling CI, Bohlmann J (2006) Genes, enzymes, and chemicals of terpenoid diversity in the constitutive and induced defence of conifers against insects and pathogens. *New Phytol* **170**: 657–675
- Kende H (1993) Ethylene biosynthesis. *Annu Rev Plant Physiol Plant Mol Biol* **44**: 283–307
- Klee HJ, Clark DG (2004) Ethylene signal transduction in flowers and fruits. In PJ Davis, ed, *Plant Hormones*. Kluwer Academic Publishers, Dordrecht, The Netherlands, pp 369–390
- Kolossova N, Miller B, Ralph S, Ellis BE, Douglas C, Ritland K, Bohlmann J (2004) Isolation of high-quality RNA from gymnosperm and angiosperm trees. *Biotechniques* **36**: 821–824
- Krokene P, Solheim H, Krokling T, Christiansen E (2003) Inducible anatomical defense responses in Norway spruce stems and their possible role in induced resistance. *Tree Physiol* **23**: 191–197
- Liang X, Abel S, Keller JA, Shen NE, Theologis A (1992) The 1-aminocyclopropane-1-carboxylate synthase gene family of *Arabidopsis thaliana*. *Proc Natl Acad Sci USA* **89**: 11046–11050
- Martin D, Bohlmann J (2005) Molecular biochemistry and genomics of terpenoid defenses in conifers. *Recent Adv Phytochem* **39**: 29–56
- Martin D, Gershenson J, Bohlmann J (2003) Induction of volatile terpene biosynthesis and diurnal emission by methyl jasmonate in foliage of Norway spruce. *Plant Physiol* **132**: 1586–1599
- Martin D, Tholl D, Gershenson J, Bohlmann J (2002) Methyl jasmonate induces traumatic resin ducts, terpenoid resin biosynthesis, and terpenoid accumulation in developing xylem of Norway spruce stems. *Plant Physiol* **129**: 1003–1018
- Martin DM, Fäldt J, Bohlmann J (2004) Functional characterization of nine Norway spruce *TPS* genes and evolution of gymnosperm terpene synthases of the *TPS-d* subfamily. *Plant Physiol* **135**: 1908–1927
- Miller B, Madilao L, Ralph S, Bohlmann J (2005) Insect-induced conifer defense: white pine weevil and methyl jasmonate induce traumatic resinosis, de novo formed volatile emissions, and accumulation of terpenoid synthase and putative octadecanoid pathway transcripts in Sitka spruce. *Plant Physiol* **137**: 369–382
- Nagy NE, Fossdal CG, Krokene P, Krokling T, Lönneborg A, Solheim H (2004) Induced responses to pathogen infection in Norway spruce phloem: changes in polyphenolic parenchyma cells, chalcone synthase transcript levels and peroxidase activity. *Tree Physiol* **24**: 505–515
- Nagy NE, Franceschi VR, Solheim H, Krokling T, Christiansen E (2000) Wound-induced traumatic resin duct development in stems of Norway spruce (Pinaceae): anatomy and cytochemical traits. *Am J Bot* **87**: 302–313
- Nehring R, Ecker JR (2004) Ethylene signal transduction in stem elongation. In PJ Davis, ed, *Plant Hormones*. Kluwer Academic Publishers, Dordrecht, The Netherlands, pp 350–368
- Page RD (1996) TREEVIEW: an application to display phylogenetic trees on personal computers. *Comput Appl Biosci* **12**: 357–358
- Pech JC, Bouzayen M, Latche A (2004) Ethylene biosynthesis. In PJ Davis, ed, *Plant Hormones*. Kluwer Academic Publishers, Dordrecht, The Netherlands, pp 115–136
- Phillips M, Bohlmann J, Gershenson J (2006) Molecular regulation of induced terpenoid biosynthesis in conifers. *Phytochemistry Reviews* **5**: 179–189
- Raffa KE, Aukema BH, Erbilgin N, Klepzig KD, Wallin KF (2005) Interactions among conifer terpenoids and bark beetles across multiple levels of scale: an attempt to understand links between population patterns and physiological processes. *Recent Adv Phytochem* **39**: 79–118
- Ralph S, Park JY, Bohlmann J, Mansfield SD (2006a) Dirigent proteins in conifer defense: gene discovery, phylogeny and differential wound- and insect-induced expression of a family of DIR and DIR-like genes in spruce (*Picea* spp.). *Plant Mol Biol* **60**: 21–40

- Ralph SG, Yueh H, Friedmann MF, Aeschliman D, Zeznik JA, Nelson CC, Butterfield YSN, Kirkpatrick R, Liu J, Jones SJM, et al** (2006b) Conifer defense against insects: microarray gene expression profiling of Sitka spruce (*Picea sitchensis*) induced by mechanical wounding or feeding by spruce budworm (*Choristoneura occidentalis*) or white pine weevils (*Pissodes strobi*) reveals large-scale changes of the host transcriptome. *Plant Cell Environ* **29**: 1545–1570
- Ramakers C, Ruijter JM, Deprez RHL, Moorman AFM** (2003) Assumption-free analysis of quantitative real-time polymerase chain reaction (PCR) data. *Neurosci Lett* **339**: 62–66
- Ro DK, Arimura GI, Lau SYW, Piers E, Bohlmann J** (2005) Loblolly pine abietadienol/abietadienal oxidase *PlAO* (CYP720B1) is a multi-functional, multi-substrate cytochrome P450 monooxygenase. *Proc Natl Acad Sci USA* **102**: 8060–8065
- Ruel JJ, Ayres MP, Lorio PL** (1998) Loblolly pine responds to mechanical wounding with increased resin flow. *Can J For Res* **28**: 596–602
- Schmidt A, Zeneli G, Hietala AM, Fossdal CG, Krokene P, Christiansen E, Gershenzon J** (2005) Induced chemical defenses in conifers. *Recent Adv Phytochem* **39**: 1–28
- Seybold SJ, Huber DPW, Lee JC, Graves AD, Bohlmann J** (2006) Pine monoterpenes and pine bark beetles: a marriage of convenience for defense and chemical communication. *Phytochemistry Reviews* **5**: 143–178
- Trapp S, Croteau R** (2001) Defensive resin biosynthesis in conifers. *Annu Rev Plant Physiol Plant Mol Biol* **52**: 689–724
- Tsuchisaka A, Theologis A** (2004) Unique and overlapping expression patterns among the *Arabidopsis* 1-amino-cyclopropane-1-carboxylate synthase gene family members. *Plant Physiol* **136**: 2982–3000
- Yamagami T, Tsuchisaka A, Yamada K, Haddon WF, Harden LA, Theologis A** (2003) Biochemical diversity among the 1-amino-cyclopropane-1-carboxylate synthase isozymes encoded by the *Arabidopsis* gene family. *J Biol Chem* **278**: 49102–49112
- Yang SF, Dong JG** (1993) Recent progress in research of ethylene biosynthesis. *Bot Bull Acad Sin (Taipei)* **34**: 89–101
- Zeneli G, Krokene P, Christiansen E, Krekling T, Gershenzon J** (2006) Methyl jasmonate treatment of mature Norway spruce (*Picea abies*) trees increases the accumulation of terpenoid resin components and protects against infection by *Ceratocystis polonica*, a bark beetle-associated fungus. *Tree Physiol* **26**: 977–988